Cooperativity and ground-state proton transfer in 7-hydroxyimidazo[1,2-a]pyridine·ammonia clusters: DFT study

ARTICLE *in* JOURNAL OF MOLECULAR STRUCTURE THEOCHEM · JANUARY 2006

Impact Factor: 1.37 · DOI: 10.1016/j.theochem.2005.10.013

3 AUTHORS, INCLUDING:

Mama Nsangou
University of Maroua
41 PUBLICATIONS **244** CITATIONS
SEE PROFILE

Nejm-Eddine Jaidane
University of Tunis El Manar
110 PUBLICATIONS **551** CITATIONS
SEE PROFILE

ELSEVIER

Journal of Molecular Structure: THEOCHEM 758 (2006) 87–95

THEO CHEM

www.elsevier.com/locate/theochem

Cooperativity and ground-state proton transfer in 7-hydroxyimidazo [1,2-a]pyridine·ammonia clusters: DFT study

M. Nsangou [a,*], N. Jaidane [b], Z. Ben Lakhdar [b]

[a] *Département de Physique, Faculté des Sciences, Université de Ngaoundéré, B.P. 454, Ngaoundéré, Cameroun*

[b] *Laboratoire de Spectroscopie Atomique, Moléculaire et Applications, Faculté des Sciences de Tunis, Campus Universitaire, 1060 Tunis, Tunisie*

Received 6 September 2005; received in revised form 27 September 2005; accepted 8 October 2005
Available online 27 December 2005

Abstract

DFT/B3LYP (6-311+G**) has been used to study twelve different geometries of 7-hydroxyimidazo[1,2-a]pyridine·$(NH_3)_n$ clusters with $n=1$–6. Ion-pair (Zwitterionic) clusters resulting from proton transfer from 7-hydroxyimidazo[1,2-a]pyridine (7HIP) to the $(NH_3)_n$ cluster have also been investigated. The structure, energetics and relative stabilities of the geometries were compared and analyzed in gaseous phase. The principle of maximum hardness has been tested by calculating chemical hardness and chemical potential to confirm the more stable of different conformers and predict their order of stability. In all cases, the solvent cluster form hydrogen bonds at –O–H or N(2) positions, or at both –O–H and N(2) positions of 7HIP. For $n=2$–4, ammonia-chain clusters are found, for $n=4$–6 other topologies appear such as cycle and mixed chain/cycle. The study of neutral forms shows that intermolecular proton transfer from the –O–H group of 7HIP to the $(NH_3)_n$ occurs for the critical size $n_c=5$ yielding a locally stable zwitterions $7HIP^- \cdot (NH_3)_4NH_4^+$. Some structural parameters such as intra- and intermolecular distances and vibrational frequency of –O–H stretching serving as indicators of proton transfer have been investigated. The natural bond orbital analysis (NBO) of the more stable conformers revealed specifically, that for a given number n of ammonia molecules, the stabilization energy $E^{(2)}$ is largest for $LP(1)N_A \rightarrow BD^*O_{15}–H_{16}$ donor–acceptor interaction ($n=2$–5), and this value increases with increasing n (22.74 kJ/mol for $n=2$, 35.38 kJ/mol for $n=3$, 35.57 kJ/mol for $n=4$ and 53.54 kJ/mol for $n=5$), showing that electron density is directly transferred to the –O–H antibonding orbital, which result in weakening and elongating of the –O–H bond and red-shift.

Keywords: 7-Hydroxyimidazo[1,2-a]pyridine; Ground-state proton transfer; Structure; DFT; B3LYP; 6-311+G**

1. Introduction

Most chemical processes of practical and biological interest take place in solution with solvent serving not only to disperse the reactants but also to provide specific solvation to reactants and products. For the last decade the influence of solvents on reactivity has been recognized. Unfortunately, less detailed information on the local structure of solvated reactants or products is available, since it is nearly impossible to isolate rapidly changing structures within the bulk of a solution [1]. A better understanding of such information may help to achieve greater control over chemical processes through the selection of appropriate solvents and reaction conditions.

One way to avoid the complexity inherent in bulk systems is to work on small clusters of reactants and solvent molecules. Recent developments in spectroscopy have shown that such clusters can be prepared experimentally in supersonic jets [2] or condensed phases [3] and studied by high resolution techniques. From a theoretical point of view, once a detailed picture of the reaction in a small cluster is obtained, several avenues are opened to generalize the results to bulk systems, two of the more promising being to increase the cluster size and to extend the study to reactions in solid matrices.

Recently, many authors [1,3–11] have discussed several solvent-assisted reactions observed in clusters with the main focus on proton transfer reactions (PTR) in *p*-CN–phenol, *p*-CHO–phenol, phenol, naphtol, 7-hydroxyquinoline and 2-hydroxypyridine/2-pyridone. The process of PTR is of fundamental and practical interest in chemistry and molecular biology [12]. The outstanding properties of PTR systems triggered an enormous interest in statistical and dynamical properties of rather small proton transfer (PT) systems having prototypical character, for instance, for large biomolecules [8]. On the other hand, intramolecular PTR in organic molecules might be considered as a simple realization of a bistable

* Corresponding author. Tel.: +237 7645210.
E-mail address: mnsangou@yahoo.com (M. Nsangou).

0166-1280/$ - see front matter © 2005 Elsevier B.V. All rights reserved.
doi:10.1016/j.theochem.2005.10.013

system. PTR are generally highly sensitive to the solvent, which makes a variety of intermolecular hydrogen bonding complexes A–H·B_n (n integer). Proton conduction through water or ammonia clusters can be studied in gas-phase. In gas-phase clusters, the occurrence of proton transfer crucially depends on the gas-phase proton affinity of the solvent molecules. In the present work, ammonia is chosen for two reasons: it is a stronger gas-phase base compared with water (their proton affinities are 853 kJ/mol and 686 kJ/mol, respectively) [13,14], and a very common solvent with its intermolecular hydrogen bonding playing a major role in the system properties. Further, a solvent with a strong gas-phase proton affinity easily scavenges protons from analyte. When a weaker gas-phase base is used instead, it is less capable of taking protons from analyte [13]. Environmental effects, i.e. interactions between acid and polar solvents, can modify the potential energy surface of the proton to a marked extent and, as a result, shift equilibrium (1) to the polar form [7,9,10].

$$AH\cdots B_n \rightarrow A^-\cdots H^+\text{–}B_n \quad (1)$$

Intramolecular PT to the B_n cluster occurs, once a critical cluster size n_c is reached. For ground- and excited-state PT, n_c depends on both the gas-phase proton acidity of the A–H and on the gas-phase proton affinity of the solvent B. Ground-state PTR have been studied experimentally and theoretically for A–H·(NH_3) clusters involving hydroxyaromatic acid A–H such as phenol [1,4], 7-hydroxyquinoline [5], *p*-CN–phenol and *p*-CHO–phenol [6], 2-hydroxypyridine [7,11] and 1-naphtol [15]. The critical size reached has been found to be $n_c = 4$ for 2-hydroxypyridine; $n_c = 5$ for *p*-CN–phenol, *p*-CHO–phenol, phenol and 7-hydroxyquinoline; and $n_c = 6$ for 1-naphtol.

Tautomeric systems such as 7-hydroxyimidazo[1,2-a]pyridine (7HIP), 2-hydroxypyridine, and 7-hydroxyquinoline are bifunctional hydrogen-bonding hydroxyaromatic molecules. They can act as proton donor at the –O–H group and as proton acceptor at the N(2) atom in the enol form (Fig. 1).

Theoretical and experimental studies on 8-hydroxyimidazo[1,2-a]pyridine were undertaken in the past by Naundorf et al. [8]. They use two Cartesian reaction coordinates to model the motion of the proton in the plane of the pyridine and imidazole, and these studies help them to discuss the applicability of various laser control scenarios to the hydroxyimidazopyridine molecule. Substituted hydroxyimidazo[1,2-a]pyridine or hydroxyimidazo[1,2-a]pyridine derivatives are extensively used for the synthesis of inhibitors which are of great interest in pharmaceutical activities [16]. The present work aims at providing a quantum chemical basis for further experimental and theoretical investigations of PT in 7HIP·$(NH_3)_n$, ($n = 1$–6) clusters, focusing on structural, energetics and harmonic frequencies aspects. In particular, optimized structures of some conformers of 7HIP·$(NH_3)_n$ are performed with focus on the search for possible PT species and the determination of the critical minimum number of ammonia molecules necessary for PT. We also investigated ion-pair (zwitterion) structure resulting from a proton transfer from the –O–H group to the $(NH_3)_n$ cluster. Structural parameters and vibrational frequencies which may serve as probes or indicators of PT are computed. This work provides the necessary systematics and insights to study further aspects of ground-state proton transfer in such systems. We also emphasize that the present work represents the first attempt of a theoretical study on solvent-assisted proton transfer in 7-hydroxyimidazo[1,2-a]pyridine, to our knowledge.

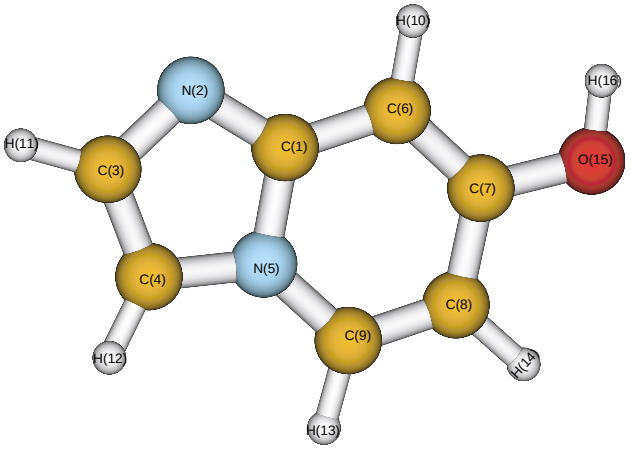

Fig. 1. Equilibrium geometry of 7-hydroxyimidazo[1,2-a]pyridine as derived from DFT/B3LYP(6-311+G**) calculations.

2. Computational methods

Calculations of the equilibrium structures and vibrational force field of 7HIP· $NH_3)_n$ clusters with up to five ammonia molecules were performed. The AM1 or PM3 semiempirical methods were first used to derive the initial structure for the following calculations. As is known from the calculations of protonated ammonia dimer [17], inclusion of electron correlation at the non-local density functional level decreases the proton barriers by a factor of 3 to 5. For this reason, geometry optimizations for all structures were carried out using the hybrid functionals Becke's three parameters (B3) [18] combined with the gradient corrected correlation functional of Lee–Yang–Parr [19]. To check that values have reached a required convergence with respect to one electron basis set size, various basis functions were tested on compound 7HIP going from 6-311G up to 6-311++G**. On the basis of these preliminary results presented in Table 1, and in order to keep the computational parameters (CPU time and disk storage) to reasonable limits and to maintain the average error under a threshold, the standard split valence triple zeta Gaussian basis set 6-311+G** of McLean and Chandler [20] with polarization functions on all atoms and diffusive functions on non-hydrogen atoms was chosen and used throughout this work. In the optimizations, both inter- and intramolecular degrees of freedom were optimized without any symmetry restriction and converged until the largest component of nuclear gradient was 10^{-6} a.u./bohr and the change in total energy was less than 10^{-7} a.u. Different cluster species are possible, but in order to sample a representative number, investigations were focused only on those that calculated vibrational frequencies gave real values, i.e. local or global minimum on the potential energy

Table 1
Some selected bond lengths and bond angles calculated at the DFT/B3LYP level of theory

Parameters	Basis sets						
	6-311G	6-311+G	6-311+G*	6-311+G**	6-311++G	6-311++G*	6-311++G**
C_1–N_2	1.341	1.342	1.326	1.325	1.342	1.326	1.326
C_1–N_5	1.421	1.420	1.407	1.407	1.420	1.407	1.407
C_1–C_6	1.413	1.413	1.414	1.415	1.413	1.414	1.415
N_2–C_3	1.387	1.387	1.367	1.368	1.387	1.367	1.368
C_3–C_4	1.377	1.378	1.374	1.374	1.378	1.374	1.374
C_4–N_5	1.396	1.396	1.386	1.386	1.387	1.386	1.386
C_6–C_7	1.373	1.373	1.372	1.372	1.373	1.372	1.372
C_7–C_8	1.427	1.426	1.425	1.425	1.426	1.425	1.426
C_8–C_9	1.363	1.364	1.361	1.361	1.364	1.361	1.361
C_9–N_5	1.379	1.379	1.370	1.370	1.379	1.370	1.370
C_7–O_{15}	1.391	1.393	1.365	1.366	1.394	1.365	1.366
O_{15}–H_{16}	0.972	0.973	0.965	0.963	0.973	0.965	0.963
C_1–N_2–C_3	105.489	105.512	105.275	105.318	105.511	105.276	105.303
N_2–C_3–C_4	111.912	111.801	112.210	112.168	111.801	112.210	112.182
N_2–C_1–N_5	110.463	110.481	111.049	111.029	110.481	111.049	111.038
C_3–C_4–N_5	105.535	105.624	105.140	105.135	105.623	105.140	105.122
N_5–C_9–C_8	119.548	119.555	119.894	119.831	119.557	119.896	119.843
N_5–C_1–C_6	118.385	118.506	118.307	118.343	118.513	118.309	118.354
C_1–C_6–C_7	119.137	118.960	119.351	119.281	118.953	119.350	119.294
C_1–N_5–C_9	121.736	121.721	121.885	121.921	121.719	121.883	121.905
C_1–N_5–C_4	106.601	106.582	106.324	106.350	106.584	106.325	106.355
C_6–C_7–C_8	121.139	121.304	120.640	120.682	121.305	120.640	120.665
C_7–C_8–C_9	120.055	119.954	119.923	119.940	119.953	119.922	119.940
C_7–O_{15}–H_{16}	112.092	112.799	110.389	109.885	112.793	110.383	109.906
O_{15}–C_7–C_8	114.931	114.857	115.447	115.459	114.851	115.443	115.458
O_{15}–C_7–C_6	123.930	123.839	123.914	123.858	123.845	123.917	123.877
[a]E	−455.0370	−455.0470	−455.1792	−455.1951	−455.0473	−455.1793	−455.1952

Computations are undertaken for seven triple zeta basis sets differing by the number of diffusive and polarization functions. Electronic energy (E) of each structure is also given.

[a] Total electronic energy.

surface. Since the importance of including the basis set superposition error (BSSE) corrections in calculated binding energies has been well documented in literature, the full counterpoise (CP) procedure of Boys and Bernadi [21] was applied to eliminate BSSE. In order to calculate the natural charges and describe some hydrogen bondings, we have used the natural bond orbital (NBO) procedure [22], implemented in the Gaussian03W computational package [23]. All the calculations have been performed on Gaussian03W computational package [23].

3. Results and discussions

3.1. Geometries

In the 7HIP·NH_3 cluster, the ammonia molecule forms a nearly linear N···HO hydrogen bond with the hydroxyl group. In its locally stable structure, optimized at the DFT/B3LYP (6-311+G**) level of theory and depicted in Fig. 2a, the hydrogen bond is calculated to be 1.843 Å. The zero point energy (ZPE), the sum of electronic energy and ZPE, the basis set superposition error (BSSE) and the counterpoise (CP)-corrected interaction energy relative to this locally stable geometry are given in Table 2.

For $n=2$, only a simple hydrogen bonded ammonia-chain cluster is formed. Its locally stable optimized geometry is shown in Fig. 2b and its CP-corrected energy presented in Table 2. This structure presents a *Cs* symmetry. The nitrogen atoms of the first and second ammonia molecules are in the plane of 7HIP. The second ammonia molecule, N_BH_3, forms two hydrogen bonds, an $N_B\cdots HN_A$ bond (2.402 Å) with the first ammonia molecule (N_AH_3) and an $N_BH\cdots N(2)$ (2.517 Å) bond with the nitrogen atom N(2) of the 7HIP molecule. The electronic energy of this structure is calculated to be −568.19 a.u in gas phase.

The 7HIP·$(NH_3)_3$ trimer can be arranged in two ways presented in Fig. 3a (III-1) and Fig. 3b (III-2). Both structures do not present a *Cs* symmetry and the relative stability between their locally stable geometries is predicted to be 3.010 kcal/mol. The lowest-energy conformation depicted in Fig. 3a, is the conformer in which the ammonia-chain links the hydroxyl group and the nitrogen atom N(2) of 7HIP. Its CP-corrected energy is −624.9819 a.u. In the less stable conformer (III-2), illustrated in Fig. 3b, the ammonia molecules form a cyclic arrangement around the hydroxyl group end, with four bent hydrogen bonds $OH\cdots N_A$, $N_AH\cdots N_B$, $N_BH\cdots N_C$ and $N_CH\cdots O$ predicted to be 1.720, 2.060, 2.146 and 2.134 Å, respectively.

In the case of 7HIP·$(NH_3)_4$ three locally stable structures have been found, see Fig. 4a (IV-1), Fig. 4b (IV-2) and Fig. 5 (IV-3). Lowest in energy is the conformer depicted in Fig. 5. This conformer is similar to the more stable structures of the trimer and dimer cases, in the sense that, the four ammonia

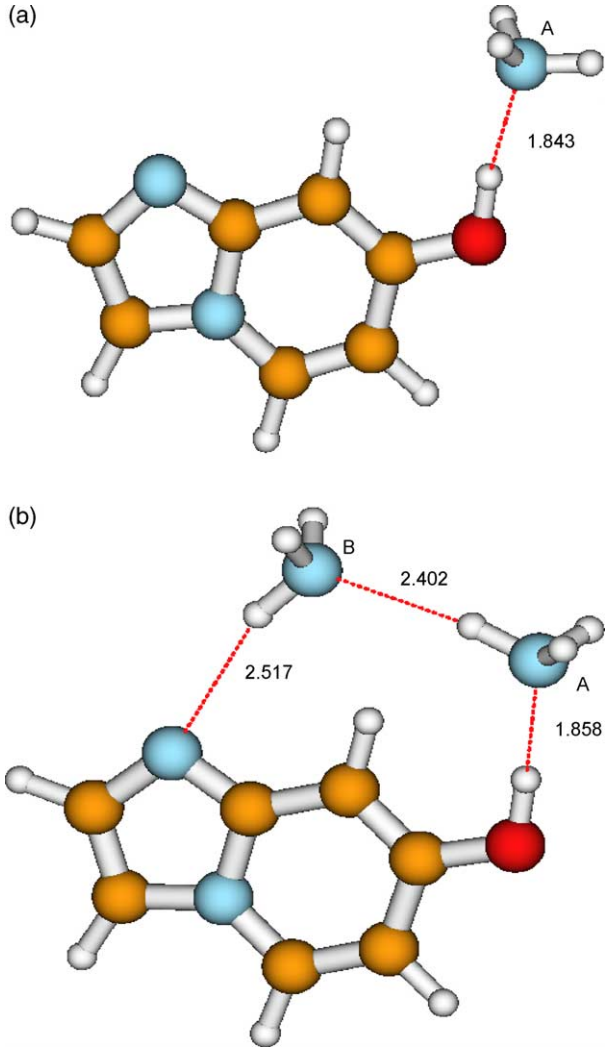

Fig. 2. Equilibrium geometries of 7HIP·(NH_3) and 7HIP·$(NH_3)_2$ as derived from DFT/B3LYP(6-311+G**) calculations.

molecules form a chain that links the oxygen and the nitrogen N(2) atoms of 7HIP. Going from oxygen to nitrogen N(2) of 7HIP, five hydrogen bonds stabilize the complex. Their values are 1.719, 2.038, 2.106, 2.120 and 2.124 Å. The second isomer (IV-2), depicted in Fig. 4b, is the intermediate (in terms of stability). It is located at 0.502 kcal/mol higher in CP-corrected energy above the most stable conformer, and at 2.132 kcal/mol lower in CP-corrected energy under the highest-energy isomer shown in Fig. 5. In the case of this second isomer, the clusters form a combination of a three-membered chain with a two-membered bifurcated-chain. Going from the hydroxyl group to the nitrogen atom N(2), the bifurcated-chain links the third ammonia molecule to the nitrogen N(2) via two hydrogen bonds $N_D\cdots HN_C$ and $N_DH\cdots N(2)$ of lengths 2.286 and 2.246 Å, while the three-membered chain is stabilized by four hydrogen bonds of lengths 1.721, 2.041, 2.097 and 2.516 Å (see Fig. 4b). The third locally stable structure, which lies at 2.132 kcal/mol higher in CP-corrected energy above the intermediate state, is formed of a four-membered cycle of ammonia molecules. This cycle goes from the –O–H group end to the oxygen atom of 7HIP. The ammonia molecules are linked by five bent hydrogen bonds 1.709, 2.042, 2.113, 2.149 and 2.127 Å (see Fig. 5).

As could be observed in Figs. 2–6 of the above-described structures, none of them exhibits a ground-state proton transfer to the $(NH_3)_n$.

For $n=5$, two different low-lying conformers depicted in Fig. 6a (V-1) and Fig. 6b (V-2) are investigated. The more stable of both conformers, denoted V-1, include a mixed chain/cycle topology. The ammonia chain links the –O–H group end and nitrogen N(2) atom, while the cycle goes from the –O–H group end to the oxygen atom. This structure which looks like the superposition of both conformers of the trimer case does not exhibit a proton transfer to the $(NH_3)_n$ cluster. Moreover, even with an extended basis set including more diffusive functions (6-311++G**) the structure's topology remains unchanged. The second pentamer, denoted V-2, less stable by 9.657 kcal/mol, is a molecular system with *Cs* symmetry. Its structure shows a proton transfer from the –O–H group of 7HIP to the closest ammonia molecule within the $(NH_3)_n$ cluster. In this system, two ammonia molecules and the protonated ammonia (NH_4^+) are located in the $7HIP^-$ molecular plane (σ_v symmetry plane). In this plane, three hydrogen bonds of lengths 1.598, 1.823 and 1.948 Å link the protonated ammonia,

Table 2
Zero point energy (ZPE) in a.u., sum of electronic energy and ZPE (E_1 in a.u.), the solvation energy (ΔE_n) in a.u., total BSSE energy, CP-corrected energy E_2 (in a.u.), dipole moment μ_M in Debye, chemical hardness η in a.u. and chemical potential μ in a.u.

Parameters	$n=0$	$n=1$	$n=2$	$n=3$		$n=4$			$n=5$	
				III-1	III-2	IV-1	IV-2	IV-3	V-1	V-2
ZPE	0.1213	0.1586	0.1965	0.2338	0.2332	0.2706	0.2705	0.2703	0.3074	0.3096
[a]E	−455.1951	−511.7942	−568.3894	−624.9861	−624.9813	−681.5762	−681.5752	−681.5719	−738.1698	−738.1544
E_1	−455.0737	−511.6356	−568.1928	−624.7523	−624.7481	−681.3056	−681.3047	−681.3016	−737.8624	−737.8449
ΔE_n		−0.0135	−0.0223	−0.0334	−0.0292	−0.0383	−0.0374	−0.0343	−0.0467	−0.0292
Δ_{BSSE}		0.0016	0.0026	0.0042	0.0038	0.0053	0.0051	0.0052	0.0064	0.0087
[b]E_2		−511.7926	−568.3867	−624.9819	−624.9774	−681.5709	−681.5701	−681.5667	−738.1634	−738.1457
μ_M	2.4150	3.2756	1.4892	1.1195	4.6646	1.1033	0.2392	4.6511	1.5754	11.9394
η	0.0840	0.0835	0.0835	0.0840	0.0825	0.0840	0.0840	0.0830	0.0830	0.0675
μ	−0.1290	−0.1135	−0.1125	−0.1130	−0.1125	−0.1130	−0.1150	−0.1120	−0.1110	−0.0855

Calculations have been done in gaseous phase ($\varepsilon=1$) using DFT/B3LYP(6-311+G**). $\eta,=(E_{LUMO}-E_{HOMO})/2$; $\mu,=(E_{LUMO}+E_{HOMO})/2$.
[a] Total electronic energy.
[b] Counterpoise corrected energy, $E_1=E+ZPE$.

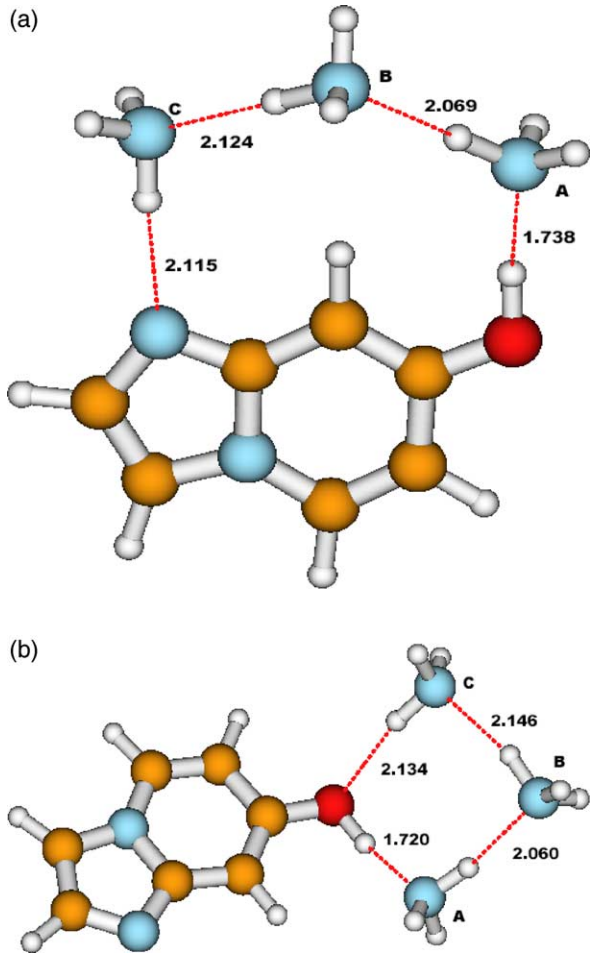

Fig. 3. Equilibrium geometries of the more stable (a) and the less stable (b) conformers of 7HIP·$(NH_3)_3$ as derived from DFT/B3LYP(6-311+G**) calculations.

NH_4^+, to oxygen via both ammonia molecules. Two other ammonia molecules (N_DH_3 and N_EH_3), located symmetrically above and below the said plane form two hydrogen bonds of equal length (1.823 Å) with the oxygen atom and two hydrogen bonds (1.732 Å) directed towards the protonated ammonia NH_4^+. In this case, there is no linkage between oxygen and nitrogen N(2) via ammonia molecules (see Fig. 6b).

For $n=6$, two different locally stable conformers are found and displayed in Fig. 7. The less stable of both structures (see Fig. 7a) is a mixed chain/cycle and looks like the superposition of Fig. 3a and Fig. 5. The more stable (see Fig. 7b) is a mixture of a chain, a cycle and a bifurcated chain. Interestingly, both structures exhibit proton transfer to the solvent, confirming that $n_c=5$ is the critical size.

3.2. Discussion

Detailed analysis of the OH···N_A hydrogen bond, in more stable structures (for $n=2$–4), show that the gradual addition of ammonia clusters leads to the strengthening of the original OH···N_A bond as evidenced by the shortening of the NO distance (2.850 Å for $n=2$, 2.741 Å for $n=3$ and 2.723 Å for $n=4$) and the lengthening of the OH bond (0.993 Å for $n=2$,

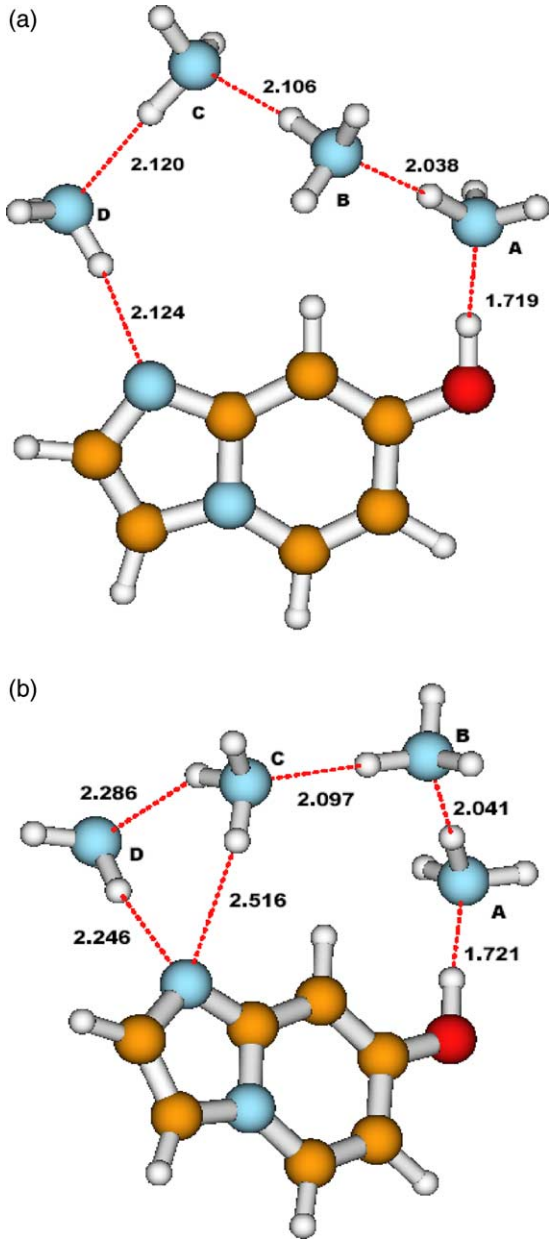

Fig. 4. Equilibrium geometries of the more stable (a) and the intermediate (b) conformers of 7HIP·$(NH_3)_4$ as derived from DFT/B3LYP(6-311+G**) calculations.

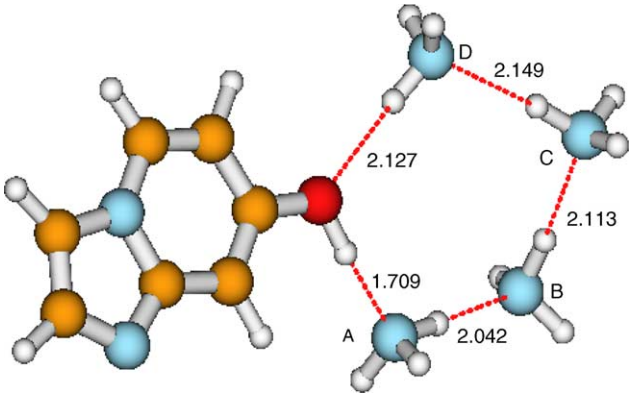

Fig. 5. Equilibrium geometry of the less stable conformer of 7HIP·$(NH_3)_4$ as derived from DFT/B3LYP(6-311+G**) calculations.

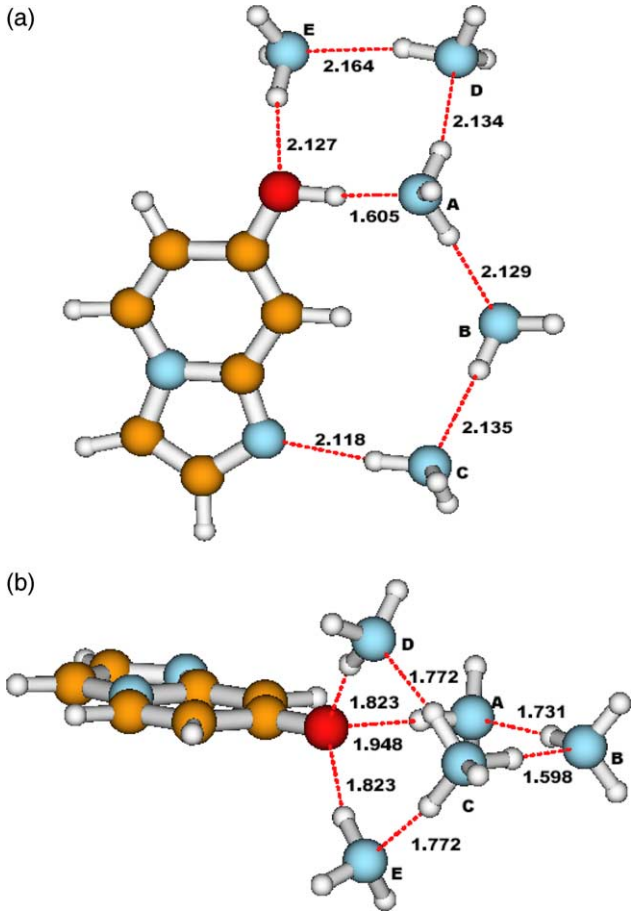

Fig. 6. Equilibrium geometries of the more stable (a) and the less stable (b) conformers of 7HIP·$(NH_3)_5$ as derived from DFT/B3LYP(6-311+G**) calculations.

1.005 Å for $n=3$ and 1.008 Å for $n=4$). Similar results were obtained in some hydroxyaromatics-ammonia clusters (phenol [1], 7-hydroxyquinoline [5] and 2-hydroxypyridine [7]). Considering the cooperativity defined as the enhancement of the first hydrogen bond between a donor and an acceptor when a second hydrogen bond is formed between one of these two species and a third partner, it is clear that the noticeably larger elongation of the –O–H bond in the tetramer complex as compared to the trimer and dimer ones indicates the strong hydrogen bond cooperativity in the said complex. The gradual change demonstrates the preparation of 7HIP for the transfer of the proton.

With respect to vibrational frequencies and IR intensities, we can see from Fig. 8 that 7HIP·$(NH_3)_n$, $n=2$–4 are IR-active and have large intensities. These IR spectral characteristics may be of great importance in the analysis of experimental features. Unfortunately, it is sometimes very difficult to predict accurate shifts in absorption intensities. For the present system, the spectra analysis indicates that most of the vibrations with strong IR intensity centralize in the fingerprint section. We mainly focus our attention on the analysis of the shifts of the OH···N_A stretch involved in the interaction of the 7HIP·$(NH_3)_n$, $n=2$–4 complexes. It turns out that the OH···N_A stretching frequency changes accordingly from 3237.7 cm^{-1} for $n=2$, 2997.0 cm^{-1} for $n=3$ and 2945.7 cm^{-1} for $n=4$, showing its strong red-shift when the second, the third and the fourth ammonia molecules are attached. The increase of the strength of the hydrogen bond (as determined by ν(–O–H) stretching frequency) is accompanied by an extremely large increase of the intensity of the stretching vibration of the proton donor (–O–H). This intensity grows from 1192.4 km/mol for $n=2$, to 2149.8 km/mol and 2394 km/mol for $n=3$ and $n=4$, respectively (see Fig. 8). It is clear that these observations are typical for classical hydrogen bonding and become more pronounced as the interaction strength increases. As the reason for the changes of the lengths and the shifts of the vibrational frequencies of –O–H bond, the most distinct contribution should be the repartition of the lone pair of electrons on the oxygen atom (O_{15}) in the OH···N_A type hydrogen bond (see Table 3).

In the NBO analysis, we focus on the stabilization energy $E^{(2)}$. This energy is calculated by the second-order perturbation theory analysis of the Fock matrix [22]. We are interested in the $E^{(2)}$ for the lone pair orbitals of the nitrogen and oxygen atoms

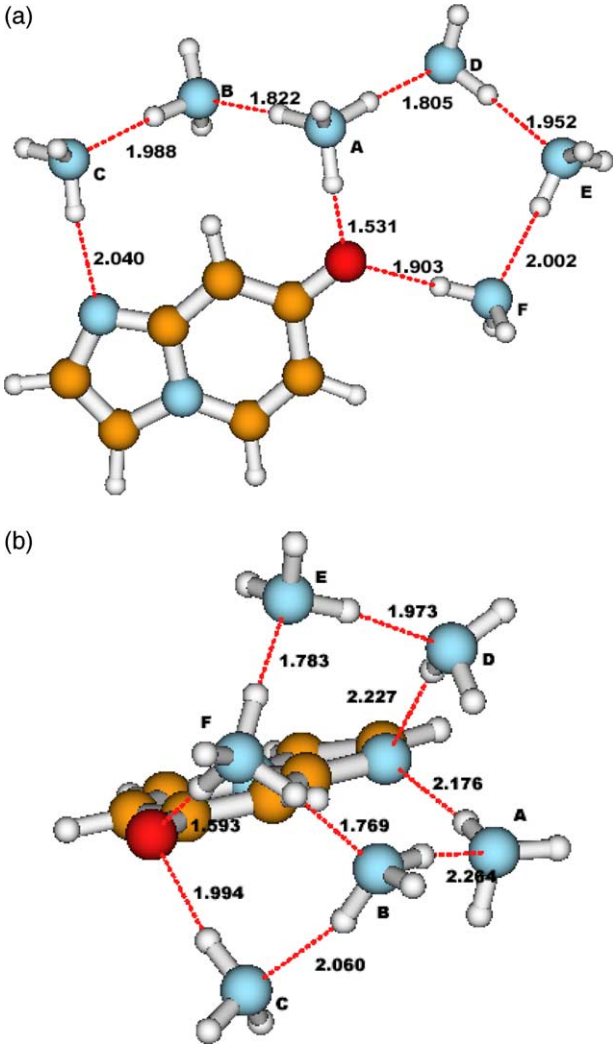

Fig. 7. Equilibrium geometries of the less stable (a) and the more stable (b) conformers of 7HIP·$(NH_3)_6$ as derived from DFT/B3LYP(6-31G*) calculations.

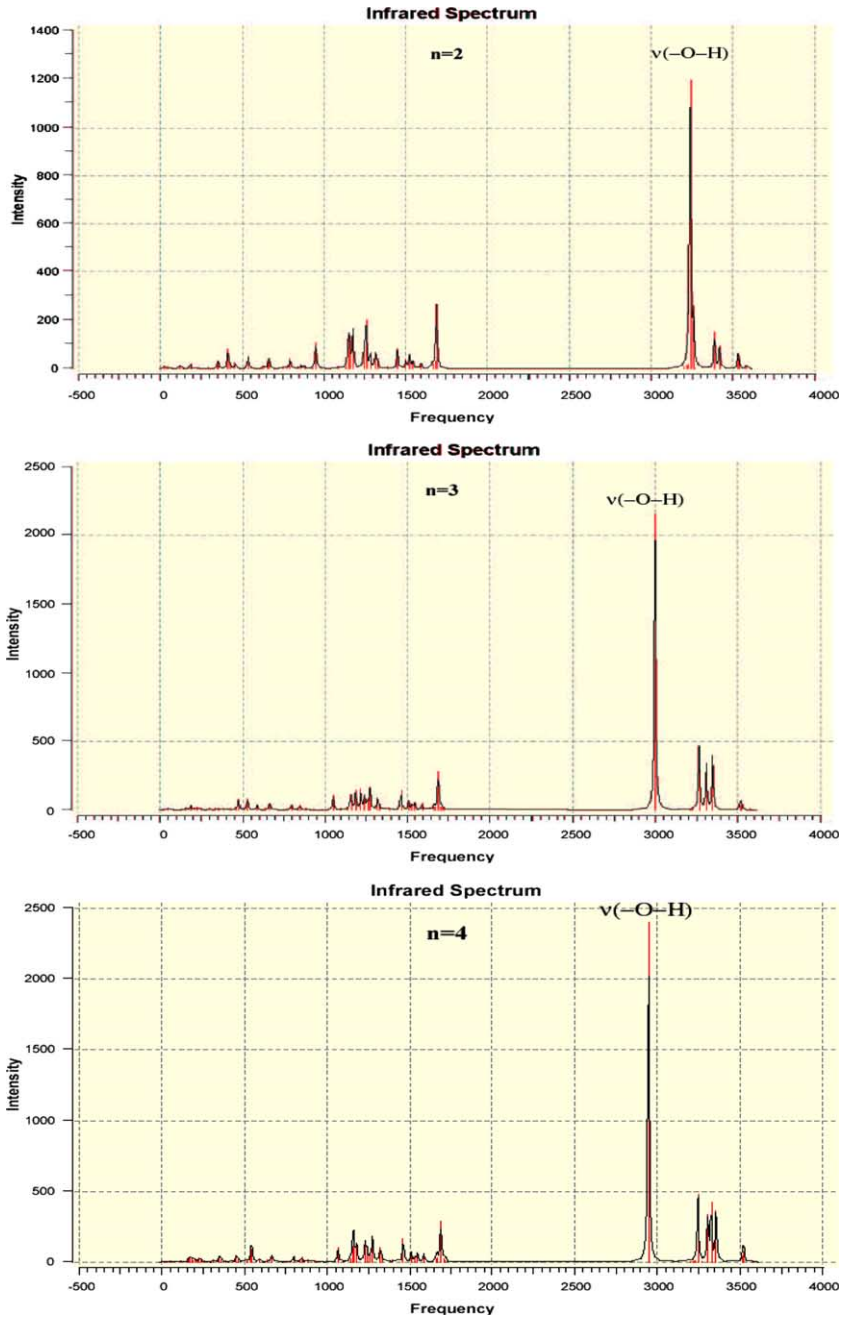

Fig. 8. Infrared spectra of most stable conformers of 7HIP·$(NH_3)_n$ $n=2$–4 as derived from DFT/B3LYP(6-311+G**) calculations.

transferred to acceptor antibonding orbitals of the –O–H and N–H bonds. Some important values of $E^{(2)}$ for the more stable complexes ($n=2$–5) are listed in Table 3. These values show that, for a given number n of ammonia molecules, $E^{(2)}$ is largest for $LP(1)N_A \rightarrow BD^*O_{15}–H_{16}$, and this value increases with increasing n (22.74 kJ/mol for $n=2$, 35.38 kJ/mol for $n=3$, 35.57 kJ/mol for $n=4$ and 53.54 kJ/mol for $n=5$) showing for these complexes that the electron density is directly transferred to the –O–H bond. These values of the stabilization energy also indicate that the electron density in the –O–H antibond orbital weakens and elongates the –O–H bond, which result in the well known red-shift of the –O–H bond stretching frequency mentioned above. Accordingly, the gradual increase of the stabilization energy may be interpreted as the preparation of the 7HIP for the proton transfer to the solvent.

The NBO results listed in Table 3 also reveal that the stabilization energy decreases in going from the hydroxyl group to the nitrogen N(2), showing that electron density is progressively transferred from the nitrogen N(2) to the –O–H antibond orbital via the ammonia chain. This observation is consistent with the progressive lengthening of the hydrogen bonds in going from hydroxyl group to the nitrogen N(2), i.e. the progressive decrease of the hydrogen bond strength.

For the above-described structures with $n=3$–5, the maximum hardness reported in Table 2 shows that the most stable conformer always corresponds to maximum hardness,

Table 3
A part of calculated second order perturbation stabilization energies $E^{(2)}$(kJ/mol) for donor–acceptor natural orbital interactions

n[a]	Donor NBO(i)	Acceptor NBO(j)	$E^{(2)}$(kJ/mol)
2	LP(1)N(A)	BD*(1)O(15)-H(16)	22.74
	LP(1)N(B)	BD*(1)N(A)-H(18)	3.34
	LP(1)N(2)	BD*(1)N(B)-H(22)	1.14
3	LP(1)N(A)	BD*(1)O(15)-H(16)	35.38
	LP(1)N(B)	BD*(1)N(A)-H(20)	10.82
	LP(1)N(C)	BD*(1)N(B)-H(24)	8.64
	LP(1)N(2)	BD*(1)N(C)-H(28)	6.29
4	LP(1)N(A)	BD*(1)O(15)-H(16)	35.57
	LP(1)N(B)	BD*(1)N(A)-H(21)	11.94
	LP(1)N(C)	BD*(1)N(B)-H(23)	8.87
	LP(1)N(D)	BD*(1)N(C)-H(25)	8.56
	LP(1)N(2)	BD*(1)N(D)-H(26)	6.14
5	LP(1)N(A)	BD*(1)O(15)-H(16)	53.54
	LP(1)N(B)	BD*(1)N(A)-H(28)	9.00
	LP(1)N(C)	BD*(1)N(B)-H(31)	8.15
	LP(1)N(D)	BD*(1)N(A)-H(26)	8.15
	LP(1)N(E)	BD*(1)N(D)-H(23)	6.79
	LP(1)O(15)	BD*(1)N(E)-H(20)	2.34
	LP(2)O(15)	BD*(1)N(E)-H(20)	1.09
	LP(1)N(2)	BD*(1)N(C)-H(34)	6.21

[a] Number of ammonia molecules in the complex.

confirming Pearson's maximum hardness principle, which states that the minimum energy structure has the maximum chemical hardness [24]. Further, for the structure V-2, the chemical hardness and chemical potential are drastically lower compared with the corresponding for the structure V-1. They are calculated to be 42.357 kcal/mol (0.0675 a.u) and −53.652 kcal/mol (−0.0855 a.u) compared with the corresponding values, 52.083 kcal/mol (0.0830 a.u) and −69.654 kcal/mol (−0.1110 a.u), for the structure V-1. These values show that the resistance of the system to charge transfer is very weak, and confirm the proton transfer observed in the geometry V-2 (ion pair) depicted in Fig. 6b. It could also be observed in this figure that intermolecular hydrogen bonding is reduced compared with those in the neutral form (see Figs. 1–6). This result is not surprising and may be explained by the fact that in neutral forms, intermolecular interactions are governed by Van der Waals ($-r^{-6}$), while in ion pair interactions decrease with r as $-r^{-4}$.

According to the solvation energies for the clustering reactions, they were calculated using the following formula

$$\Delta E_n = E_{7\ \mathrm{HIP}\cdots(\mathrm{NH_3})_n} - E_{7\ \mathrm{HIP}} + nE_{\mathrm{NH_3}},$$

in which energies were ZPE-corrected. These values reported in Table 2, confirm the order of stability of each isomer for $n=2$–5. The more stable isomer always corresponds, in absolute values, to the maximum solvation energy. These values also show that proton transfer to the solvent is endoergic by 18.323 kcal/mol (0.0292 a.u), for V-2 structure.

4. Conclusion

Twelve different 7HIP·$(NH_3)_n$, $n=1$–6 clusters were investigated at the DFT/B3LYP (6-311+G**) level of theory. To our knowledge, these calculations represent the first attempt to study the structures and energies of these complexes, in gaseous phase, near the PT threshold in ground-state. The existence of locally stable enol conformers and zwitterion forms was established. The DFT/B3LYP (6-311+G**) calculations indicate that enol sizes with $n\leq 4$ cannot give rise to proton transfer in the electronic ground-state. It is found that the critical size $n_c=5$ is the smallest species for which proton transfer within the cluster may occur. Moreover, it appears that some structural parameters (inter- and intra-molecular distances) and vibrational frequencies drastically change at this particular critical size, serving as indicators of proton transfer to the solvent. It is also clear that the lengthening of the –O–H bond accompanied by a red shift and intensity increase of the –O–H stretch are the major effects of complexation on the 7HIP ammonia clusters properties. Proton transfer to the solvent can then be predicted by characterization of several parameters as a function of the cluster size.

The maximum hardness confirms the more stable isomer and predict their order of stability.

Acknowledgements

The authors are thankful to Dr. M. Taieb Ben Dhia, Department of Chemistry, University Tunis El Manar, Tunisia, for supplying the Gaussian 03W software package. One of the authors (M.N.) is highly indebted to Prof. Zohra Ben Lakhdar for her warm hospitality and scientific support during his stay in Tunisia. He also thanks the Abdus Salam ICTP (Trieste, Italy), Office of External Activities, for their financial support (Grant No. LIBS-OEA-NET 45).

References

[1] W. Siebrand, M.Z. Zgierski, Z.K. Smedarchina, M. Vener, J. Kaneti, Chem. Phys. Lett. 266 (1997) 47.
[2] A. Iwasaki, M. Fujii, T. Watanabe, T. Ebata, N. Mikami, J. Phys. Chem. 100 (1996) 16053; F. Lahmani, A. Douhal, E. Breheret, A. Zehnacker-Rentien, Chem. Phys. Lett. 220 (1994) 235.
[3] M. Bonn, M.J.P. Brugmans, A.W. Kleyn, R.A. van Santen, H.J. Bakker, Phys. Rev. Lett. 76 (1996) 2440.
[4] C. Crépin, A. Tramer, Chem. Phys. 156 (1991) 281; M. Vener, Chem. Phys. 233 (1998) 77; S. Matrenchard, C. Dedonder, C. Jouvet, D. Sogaldi, M. Vervloet, C. Grégoire, I. Dimicoli, Chem. Phys. Lett. 310 (1999) 173; S.-I. Ishiuchi, K. Daigoku, M. Saeki, M. Sakai, K. Hashimoto, M. Fujii, J. Chem. Phys. 117 (2002) 7077; S.-I. Ishiuchi, K. Daigoku, M. Saeki, M. Sakai, K. Hashimoto, M. Fujii, J. Chem. Phys. 117 (2002) 7083.
[5] A. Bach, S. Leutwyler, J. Chem. Phys. 112 (2000) 560; S. Coussan, M. Meuwly, S. Leutwyler, J. Chem. Phys. 114 (2001) 3524; A. Bach, C. Tanner, C. Manca, H.M. Frey, S. Leutwyler, J. Chem. Phys. 119 (2003) 5933.
[6] M.V. Vener, S. Iwata, Chem. Phys. Lett. 292 (1998) 87.
[7] M. Esboui, M. Nsangou, N. Jaidane, Z. Ben Lahkdar, Chem. Phys. 311 (2005) 277.
[8] H. Naundorf, J.A. Organero, A. Douhal, O. Kühn, J. Chem. Phys. 110 (1999) 11286; S.K. Douhal, A. Kim, A. Zewail, Nature (Lond.) 378 (1995) 260.
[9] E.A. Pshenichnov, N.D. Sokolov, Int. J. Quant. Chem. 1 (1967) 855.

[10] Th. Zeegers-Huyskens, P. Huyskens, in: H. Ratajczak, W.J. Orville-Thomas (Eds.), Molecular Interactions, vol. 2, Wiley, New York, 1981, pp. 47–49.
[11] C. Adamo, V. Barone, S. Loison, C.J. Minichinio, Chem. Soc. Perkin Trans. 2 (1993) 267; A.L. Sobolewski, Chem. Phys. Lett. 211 (1993) 293; V. Barone, C. Adamo, Chem. Phys. Lett. 226 (1994) 399; J.E. Del Bene, J. Am. Chem. Soc. 117 (1995) 1607; A.L. Sobolewski, L. Adamowicz, J. Phys. Chem. 100 (1996) 3933; P.T. Chou, C.Y. Wei, F.T. Hung, J. Phys. Chem. B 101 (1997) 9119; A. Dkhissi, L. Adamowicz, G. Maes, J. Phys. Chem. A 104 (2000) 5625.
[12] T. Bountis, Proton Transfer in Hydrogen-bonded Systems, Plenum, New York, 1992; D. Hadzi, Theoretical Treatments of Hydrogen Bonding, Wiley, New York, 1997.
[13] S.G. Lias, J.F. Liebman, R.D. Levin, J. Phys. Chem. Ref. Data 13 (1984) 695.
[14] M.H. Amad, N.B. Cech, G.S. Jackson, C.G. Enke, J. Mass Spectrom. 35 (2000) 784; J.F. Gal, P.C. Maria, E.D. Raczynska, J. Mass Spectrom. 36 (2001) 699.
[15] M.F. Hineman, D.F. Kelley, E.R. Bernstein, J. Phys. Chem. 97 (1992) 3341; W. Siebrand, M.Z. Zgierski, Chem. Phys. Lett. 320 (2000) 153.
[16] J.A. Watts, A. Watts, D.A. Middleton, J. Biol. Chem. 276 (2001) 43197.
[17] S. Ikuta, J. Chem. Phys. 87 (1987) 1900; L. Jaroszewski, B. Leysing, J.T. Tanner, J.A. McCammon, Chem. Phys. Lett. 175 (1990) 282; S. Sadukhan, D. Munoz, C. Adamo, G.E. Scuseria, Chem. Phys. Lett. 306 (1999) 83.
[18] A.D. Becke, Phys. Rev. A 38 (1998) 3098.
[19] C. Lee, W. Yang, R.G. Parr, Phys. Rev. B 37 (1988) 785.
[20] A.D. McLean, G.S. Chandler, J. Chem. Phys. 72 (1980) 5639; R. Krishnan, J.S. Binkley, R. Seeger, J.A. Pople, J. Chem. Phys. 72 (1980) 650.
[21] S.F. Boys, F. Bernadi, Mol. Phys. 19 (1970) 553.
[22] A.E. Reed, R.B. Weinstock, F. Weinhold, J. Chem. Phys. 83 (1985) 735; E.D. Glendening, A.E. Reed, J.E. Carpenter, F. Weinhold, NBO Version 3; A.E. Reed, L.A. Curtiss, F. Weinhold, Chem. Rev. 88 (1988) 899; F. Weinhold, J.E. Carpenter, Plenum, 1988, p. 227.
[23] M.J. Frisch, G.W. Trucks, H.B. Schlegel, G.E. Scuseria, M.A. Robb, J.R. Cheeseman, J.A. Montgomery Jr., T. Vreven, K.N. Kudin, J.C. Burant, J.M. Millam, S.S. Iyengar, J. Tomasi, V. Barone, B. Mennucci, M. Cossi, G. Scalmani, N. Rega, G.A. Petersson, H. Nakatsuji, M. Hada, M. Ehara, K. Toyota, R. Fukuda, J. Hasegawa, M. Ishida, T. Nakajima, Y. Honda, O. Kitao, H. Nakai, M. Klene, X. Li, J.E. Knox, H.P. Hratchian, J.B. Cross, C. Adamo, J. Jaramillo, R. Gomperts, R.E. Stratmann, O. Yazyev, A.J. Austin, R. Cammi, C. Pomelli, J.W. Ochterski, P.Y. Ayala, K. Morokuma, G.A. Voth, P. Salvador, J.J. Dannenberg, V.G. Zakrzewski, S. Dapprich, A.D. Daniels, M.C. Strain, O. Farkas, D.K. Malick, A.D. Rabuck, K. Raghavachari, J.B. Foresman, J.V. Ortiz, Q. Cui, A.G. Baboul, S. Clifford, J. Cioslowski, B.B. Stefanov, G. Liu, A. Liashenko, P. Piskorz, I. Komaromi, R.L. Martin, D.J. Fox, T. Keith, M.A. Al-Laham, C.Y. Peng, A. Nanayakkara, M. Challacombe, P.M.W. Gill, B. Johnson, W. Chen, M.W. Wong, C. Gonzalez, J.A. Pople, GAUSSIAN 03, Revision B.05, Gaussian, Inc., Pittsburgh, PA, 2003.
[24] R.G. Pearson, Hard and Soft Acids and Bases, Dowden (Hutchinson & Ross), Strodsburg, PA, 1973.